JOURNAL OF MATERIALS SCIENCE 27 (1992) 1428–1434

Analysis of the role of adhesion in composites that contain particles

J. S. FURNO, E. B. NAUMAN
Department of Chemical Engineering, Rensselaer Polytechnic Institute, Troy, NY 12180–3590, USA

The role of adhesion in rubber modified polymers was determined using finite element stress analysis. Adhesion between the two phases was found to be unimportant in terms of the stress concentrations in the matrix phase, even near the polymer–rubber interface. By considering zero adhesion and perfect adhesion limits, bounds on the interfacial behavior have been established. The stress analysis predicts elastic properties such as modulus, Poisson's ratio and yield strength. A comparison is made to experimental results on a thermoplastic/elastomer blend.

1. Introduction

The impact modification of polymers is possible through incorporation of rubbery phase domains into an otherwise brittle polymer matrix. High-impact polystyrene (HIPS), acrylonitrile–butadiene–styrene (ABS), and modified epoxies are well known and important materials that employ this technique. Increases in the toughness of glassy polymers with the addition of rubber particles is believed to be due to the rubber particles ability to induce wide-spread energy-absorbing deformation processes, such as crazing and shear yielding, in the matrix material during fracture [1]. Researchers have shown that rubber inclusions cause a local stress magnification in the matrix material immediately surrounding the inclusion [2, 3]. This local stress magnification is believed to initiate crazing and shear yielding. Goodier [2] provided an analytical solution for the internal stresses surrounding a single inclusion in an infinite matrix subjected to a uniaxial tension. Broutman and Panizza [3] later developed a numerical method using finite element analysis to account for interactions between particles in a multi-particle composite material. Liu and Nauman [4] found the exact solution for the stress distribution within the inclusion for the single particle problem. In all the previous work [2–8] the assumption of perfect adhesion (continuity of displacements) between the inclusion and the matrix has been used. Much debate exists in the literature over the importance of adhesion and the degree of adhesion between the rubber and polymer phases to the final composite properties, especially impact resistance [1, 4, 9–14]. In this work, we examine the effect of interfacial bonding on the composite behaviour by eliminating the perfect adhesion assumption. Instead, we consider the case where the matrix and rubber act as two separate entities that have no interfacial forces holding them together. We would expect a real composite system to behave intermediately to these two extremes.

Here we consider the effect of inclusion modulus and inclusion volume fraction using the two different interface conditions. In addition, the internal stress analysis is used to predict elastic properties such as modulus, Poisson's ratio and yield strength. These results are compared to the experimental findings of Furno and Nauman [15].

2. Finite element stress analysis

The application of the finite element method to stress analysis has been well documented [16, 17]. For completeness, a brief description of the method will be given here. A structure is first divided into a set of discrete elements. The boundaries of the elements are defined as straight lines between nodal points. These nodes are common points which interconnect the elements in the discretized system. When the structure is subjected to a given set of boundary conditions, the displacement at each node and the stresses in each element can be evaluated by solving the equilibrium equations along with the continuity relations between the elements.

Following the work of Broutman and Panizza [3], the analysis was performed in cylindrical coordinates on an axisymmetric solid. The model system consists of a sphere embedded in a cylinder which has periodic boundary conditions at its outer surface. As recognized by the original workers, this model does not accurately define an actual repetitive unit. It does, however, provide an accurate description with respect to the volume fraction of modifier and the interparticle spacing. Agarwal and Broutman [18] compared their results with those from a full three-dimensional analysis for an alumina-filled glass. They concluded that the small differences between the two approaches did not warrant the added expense and complexity of the three-dimensional analysis.

The finite element package ABAQUS was used to solve this composite stress analysis problem. Boyce

0022–2461

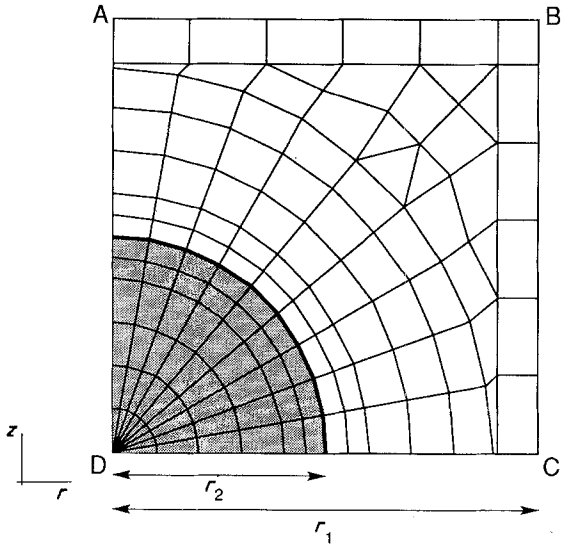

Figure 1 Finite element grid $(r_2/r_1) = 0.5 = 8.3\%$ rubber.

et al. [8] previously used the same package to analyse the internal stresses of composites containing layered spherical inclusions and thermal residual stresses. One of the finite element grids used in the present work is given in Fig. 1. The grid shown is for the case where the composite contains an 8.3% volume fraction of modifier $(r_2/r_1 = 0.5)$. The volume fraction and interparticle spacing in the model are given by

$$\text{volume fraction} = \tfrac{2}{3}(r_2/r_1)^3 \quad (1)$$

$$\text{interparticle spacing} = 2(r_1 - r_2) \quad (2)$$

where r_1, the cell length, and r_2, the particle radius, are depicted in Fig. 1.

Whereas previous workers considered perfect bonding to exist between the inclusion and the matrix, we also considered the case where there is no adhesion between the two phases. In the finite element method, this no adhesion case was modelled by supposing that a gap interface exists between the outer elements of the inclusion and the adjacent matrix elements. The width of the gap was reduced until there was no longer an effect on the stress analysis results. In essence, a numerically infinitesimal gap was used to model the lack of adhesive forces between the inclusion and matrix. As a result, only compressive forces and not tensile or shear forces are transmitted from the matrix to the inclusion. In contrast, the perfect adhesion assumption provides perfect transmission of tensile and shear forces as well as compressive forces.

The boundary conditions and solution procedure used follows that of Broutman and Panizza. The region ABCD as shown in Fig. 1 is subjected to a uniaxial tension in the z-direction, only. This tension results in a stretching of the cell in the z-direction with a corresponding contraction in the r-direction related to the Poisson's ratio of the composite. By symmetry, the shear stress, τ_{rz}, on the boundary must be zero, thus sides AB and BC remain parallel to their original position while AD and DC remain fixed. In addition, no external force is acting on the boundary BC so that

$$\int_{BC} \sigma_r \, dz = 0 \quad (3)$$

These boundary conditions are satisfied by the superposition of two separate stress analysis problems. In the first problem, the cell is given zero displacements on all boundaries except for the top (AB) which is subjected to a unit (positive) displacement in the z-direction. The second stress and displacement distribution is calculated subject to zero displacements on all sides except for, this time, the right side (BC) which is subjected to a unit normal displacement (r-direction). The two stress and displacement distributions are then superimposed by

$$\sigma = \sigma_1 + k\sigma_2 \quad (4)$$

$$u = u_1 + ku_2 \quad (5)$$

where k is evaluated such that boundary condition 3 is satisfied

$$\int_{BC} (\sigma_{r_1} + k\sigma_{r_2}) dz = |BC|(\bar{\sigma}_{r_1} + k\bar{\sigma}_{r_2}) = 0 \quad (6)$$

so

$$k = -\left(\frac{\bar{\sigma}_{r_1}}{\bar{\sigma}_{r_2}}\right)_{BC} \quad (7)$$

The necessity for calculating and superimposing two separate distributions is due to the fact that the composite Poisson's ratio is not known *a priori*, but instead must be evaluated. Equations 3, 6 and 7 allow for the evaluation of the Poisson's ratio as

$$\nu = |k| \quad (8)$$

The result of this analysis is the stress and displacement distributions throughout the matrix and inclusion for a composite material that is put under a uniaxial tension in the z-direction of magnitude equal to

$$\bar{\sigma}_z = \frac{\int_A \sigma_z \, dA}{A} \quad (9)$$

where

$$\int_A \sigma_z \, dA = 2\pi \int_0^{r_1} \sigma_z r \, dr = \pi \sum_{i=1}^{n} (r_i^2 - r_{i-1}^2)\sigma_z \quad (10)$$

and where A is the top (circular) surface of the cylindrical axisymmetric cell.

The stress distribution found in this manner is in cylindrical coordinates. The stress components can be transformed into the more familiar spherical coordinate system using the following transformations

$$\sigma_y = \sigma_\theta = \sigma_z \cos^2\theta + \sigma_r \sin^2\theta - \tau_{rz} \sin 2\theta \quad \text{(hoop stress)} \quad (11)$$

$$\sigma_x = \sigma_{rr} = \sigma_z \sin^2\theta + \sigma_r \cos^2\theta + \tau_{rz} \sin 2\theta \quad \text{(radial stress)} \quad (12)$$

$$\sigma_t = \sigma_{\psi\psi} = \sigma_\phi \quad \text{(tangential stress)} \quad (13)$$

$$\tau_{xy} = \tau_{r\theta}$$
$$= \tau_{rz}\cos 2\theta - \tfrac{1}{2}(\sigma_r - \sigma_z)\sin 2\theta \quad \text{(shear stress)} \tag{14}$$

These components of stress can then be used to calculate the Mise's equivalent stress within the material. This equivalent stress gives us a better appreciation of the magnitude of the triaxial stresses acting locally in the composite which can induce deformation. The Mise's equivalent stress is calculated as

$$\sigma_E = \{\tfrac{1}{2}[(\sigma_1 - \sigma_2)^2 + (\sigma_2 - \sigma_3)^2 + (\sigma_3 - \sigma_1)^2]\}^{1/2} \tag{15}$$

where σ_1, σ_2, and σ_3 are the principal stresses and σ_E is the Mise's equivalent stress.

In addition to Poisson's ratio, Broutman and Panizza [3] describe how other elastic properties of the composite, such as the modulus of elasticity, can be calculated from the stress and displacement distributions. The modulus of elasticity is defined as

$$E = \frac{\bar{\sigma}_z}{\bar{\varepsilon}_z} \tag{16}$$

where $\bar{\varepsilon}_z$ is the strain in the z-direction. The stress, $\bar{\sigma}_z$, is evaluated from Equations 9 and 10. The strain is calculated from the prescribed displacement of the AB boundary as

$$\bar{\varepsilon}_z = \frac{(u_z)_{AB}}{|BC|} \tag{17}$$

The model calculations also allow prediction of the yield strength. The yield strength is the stress at which the composite begins to experience widespread, non-recoverable yielding. This occurs when entire cross-sections of material perpendicular to the applied tension begins to yield. The yield strength of the unmodified matrix material is given as σ_M^*. Yielding in the composite material would thus begin at some entire cross-section that first experiences an equivalent stress greater than σ_M^*. This first yielding cross-section would be defined as the cross-section that has the largest minimum stress of all matrix cross-sections. From this, we can then calculate the yield strength of the composite as

$$\sigma_c^* = \sigma_M^*\left[\frac{\max(\sigma_{x_{min}})}{(\bar{\sigma}_z)_{AB}}\right] \tag{18}$$

where $\sigma_{x_{min}}$ is the minimum equivalent stress in the matrix phase along any given cross-section perpendicular to the applied tension.

In order to ensure the accuracy of the finite element stress analysis for both the perfect adhesion and no adhesion cases, a number of tests were conducted on the models. First of all, the analysis using the perfect adhesion assumption was used to reproduce the results of Broutman and Panizza [3]. Increases in the number of elements were shown to have negligible effect on the results of the stress analysis. Two limiting cases were also tested. The first case assigned the inclusion properties identical to those of the matrix. For the perfect adhesion results, the internal stresses were found to be equal throughout the volume (and equal to the applied tension) as expected for an isotropic homogeneous material. In addition, the elastic properties calculated from the stress field were equal to the matrix properties. The second limiting case used for model verification was the limit of decreasing inclusion modulus. For very low inclusion moduli, the results obtained from the no adhesion model are the same as those for perfect adhesion. This result is intuitively correct because the limit of decreasing inclusion modulus is a void in the material, and for this case the two models should be identical.

3. Results and discussion

We first consider a composite material containing 8.3% rubber dispersed in a glassy matrix. The com-

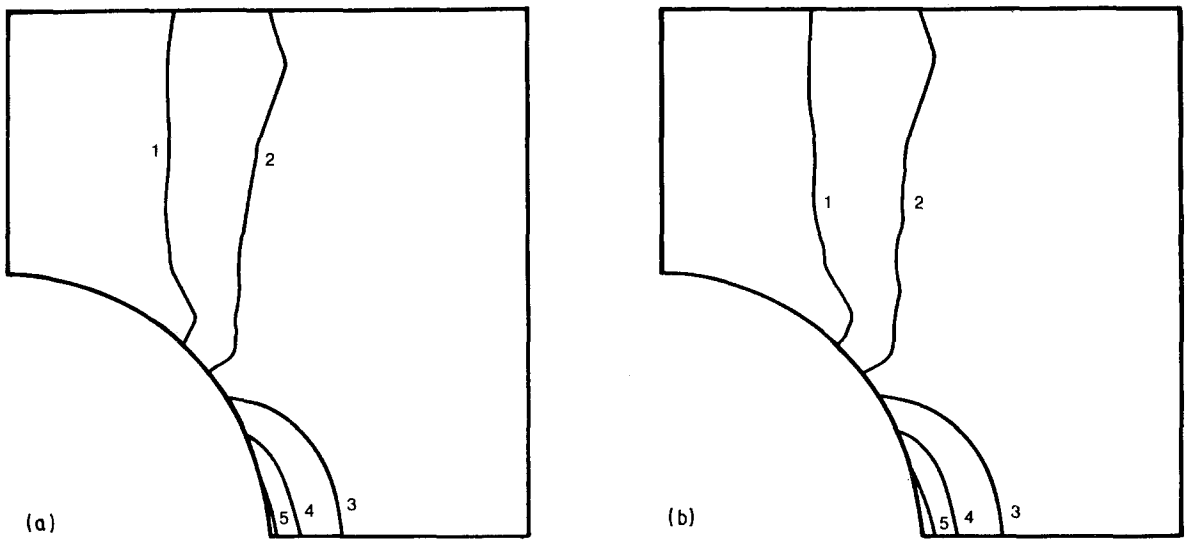

Figure 2 Distribution of Mise's equivalent stress in the matrix around a rubber particle (8.3% modifier): (a) perfect adhesion, (b) no adhesion. $\sigma_E/\bar{\sigma}_z$: (1) 0.075, (2) 1.00, (3) 1.25, (4) 1.50, (5) 1.75.

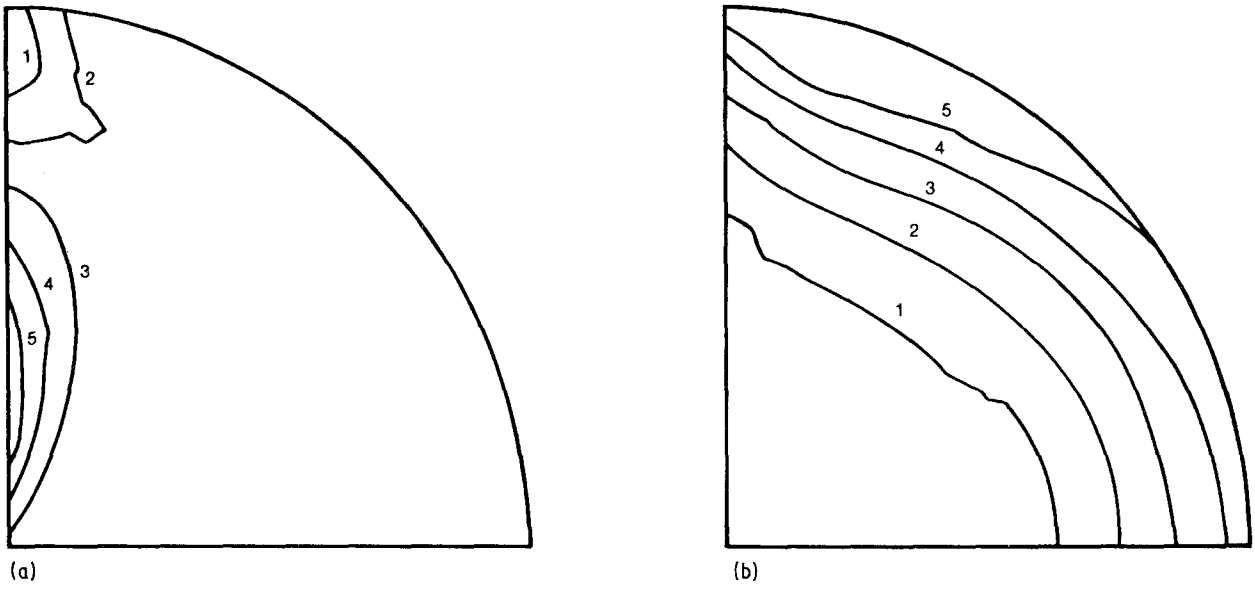

Figure 3 Distribution of Mise's equivalent stress in the rubber particle of a rubber-modified polymer (8.3% modifier): (a) perfect adhesion, (b) no adhesion. $\sigma_E/\bar{\sigma}_z$: (a) (1) 0.010, (2) 0.012, (3) 0.014, (4) 0.016, (5) 0.018; (b) (1) 0.010, (2) 0.020, (3) 0.030, (4) 0.040, (5) 0.050.

ponent properties are

polymer: $E = 400\,000$ p.s.i. (10^3 p.s.i. $= 6.89$ N mm^{-2})

$\nu = 0.35$

rubber: $E = 3000$ p.s.i.

$\nu = 0.48$

These values are similar to those used by Broutman and Panizza [3]. Fig. 2 shows contour plots of the Mise's equivalent stress in the matrix phase of the composite for both the perfect adhesion and no adhesion cases. The difference in interfacial adhesion has virtually no effect on the stress state of the matrix. Thus the level of adhesion of a rubber particle to the surrounding matrix is unimportant in terms of the particle's ability to act as a local stress intensifier and to initiate energy-absorbing deformation processes, such as crazing and shear yielding.

This, however, does not mean that a non-bonded rubber particle will be an effective impact modifier for a polymer. To consider this, we appeal to fracture mechanics arguments instead of stress analysis. Specifically, we need to know if the lack of adhesion provides a flaw of critical size which would initiate premature fracture instead of energy absorbing deformation. One could argue that there exists particles small enough or adhesion levels high enough (more realistically, a combination of the two) such that critical flaws are not present to cause premature failure. The experimental work of Furno and Nauman [19], Nauman *et al.* [12] and Wu [9] seems to support this idea.

Contour plots of the Mise's equivalent stress inside the spherical rubber inclusion for the perfect adhesion and no adhesion case are shown in Fig. 3. Unlike the matrix, the rubber phase experiences a vastly different stress field depending on the interfacial bonding. The difference in stress states of the rubber for the extremes in adhesion is due to the forces that are transmitted to the particle. For the perfect adhesion case, tensile, compressive, and shear stresses are perfectly transmitted to the rubber particle whereas in the no adhesion case, the particle only receives compressive forces applied by the matrix.

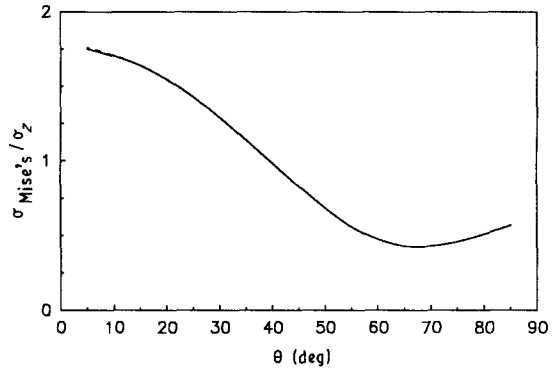

Figure 4 Internal stress intensity factor as a function of position about a particle of modulus 3 p.s.i. (8.3% modifier). (—) Perfect adhesion, (– – –) no adhesion.

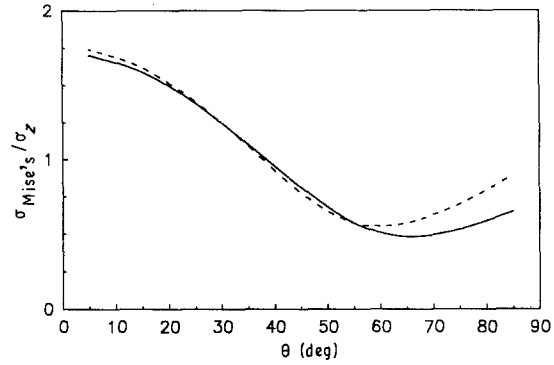

Figure 5 Internal stress intensity factor as a function of position about a particle of modulus 3000 p.s.i. (——) Perfect adhesion, (– – –) no adhesion.

Figs 4–6 show the interfacial stress intensity factor within the matrix for both the perfect and no adhesion cases as a function of position about the rubber particle for inclusion moduli of 3, 3000 and

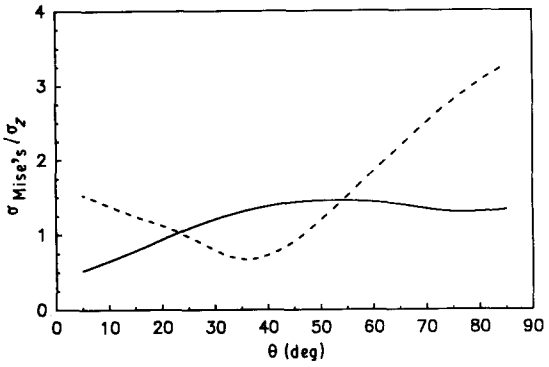

Figure 6 Internal stress intensity factor as a function of position about a particle of modulus 3.0×10^6 p.s.i. (——) Perfect adhesion (---) no adhesion.

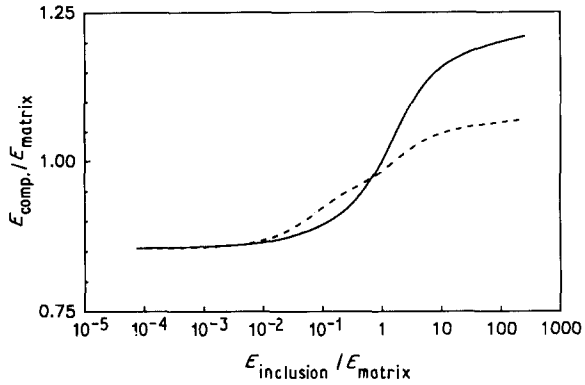

Figure 7 Predicted composite modulus as a function of inclusion modulus (8.3% modifier). (—) Perfect adhesion, (---) no adhesion.

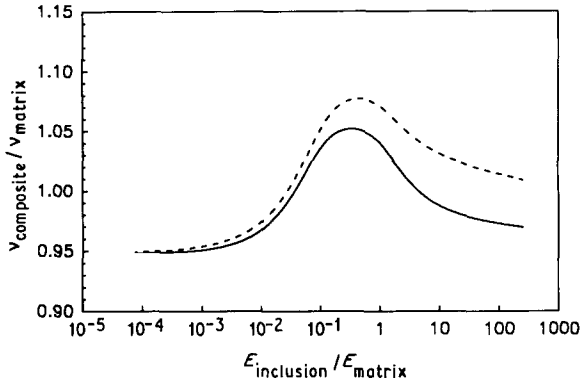

Figure 8 Predicted composite Poisson's ratio as a function of inclusion modulus (8.3% modifier). (—) Perfect adhesion, (---) no adhesion.

3.0×10^6 p.s.i. respectively. The other matrix and inclusion properties are the same as those in the previous example. The reader should take some caution in interpreting these results because the Poisson's ratio of the inclusion may be physically unrealistic for the given modulus, especially for the high modulus inclusion cases. Broutman and Panizza [3], however, found that the analysis is insensitive to changes in Poisson's ratio. For extremely low modulus inclusions, the stress field in the matrix is almost identical for both interfacial conditions and converges to the solution of a material containing spherical voids. Fig. 5 shows that only minor differences exist between the perfect adhesion and no adhesion cases in terms of stress magnification about the inclusion. This figure is most indicative of the situation for a rubber-modified thermoplastic. A maximum is predicted by both models at the equator of a particle ($\theta = 0$) perpendicular to the applied stress. This result is consistent with the experimental observation that crazes, which are responsible for increased strength in many rubber modified polymers, are initiated at the equator of the rubber particle.

Fig. 6 shows that the perfect adhesion and no adhesion assumptions result in vastly different stress fields when the inclusion is stiffer than the matrix. Not only is the magnitude of the stress magnification different for the two models, but so is the location of the maximum stress about the particle. The no adhesion assumption results in a predicted maximum in stress to occur at the particle axis parallel to the applied stress. In contrast, the maximum equivalent stress at $r = r_2$ for the perfect adhesion model occurs approximately 50° from the particle equator. Wang *et al.* [20] found that crazes originated, on average, 53° from the inclusion equator when a macro-composite consisting of a steel ball (surface-treated for good adhesion) in a polystyrene matrix was subjected to a uniaxial tension. In addition, Dekkers and Heikens [21] found that shear bands formed under tension at $\theta = 45°$ about glass beads that were well bonded to a polycarbonate matrix. Poorly bonded beads resulted in dewetting at the poles followed by shear band formation between the poles and equator. The highest stress concentration predicted using the perfect adhesion assumption, however, occurs a small distance away from the particle surface at $\theta = 90°$. This, perhaps, explains Dekkers and Heikens [5] observation of crazes at the poles of glass beads that were well bonded to a polystyrene matrix and subjected to uniaxial tension. Dekkers and Heikens [5, 21] results suggest that different mechanisms are operative in craze and shear band formation. As noted by Wang *et al.* [20] and Dekkers and Heikens [21] for perfectly adhering hard particles, maxima in major principal stress and dilation occur at the poles of the inclusion while maxima in major principal strain, strain energy density, major principal shear stress, and distortion strain energy density (similar to Mise's equivalent stress) occur near $\theta = 45°$. Using the no adhesion model, the maximum value of all of these quantities occurs at $\theta = 90°$.

Using the methods described by Broutman and Panizza [3], the elastic properties of the composite can be calculated from the stress analyses. Figs 7 and 8 show the calculated composite modulus and Poisson's ratio, respectively, as a function of inclusion modulus. The predicted elastic properties of the composite are nearly the same for both adhesion models until the modulus of the inclusion approaches or surpasses the modulus of the matrix. This means that the composite elastic properties (of rubber-modified thermoplastics) are insensitive to the degree of adhesion between the matrix and inclusion.

Let us now consider the effect of increasing rubber content on the properties of an impact-modified poly-

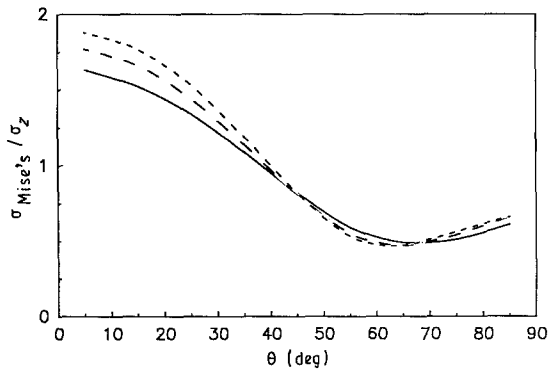

Figure 9 Interfacial stress intensity factor as a function of position about the rubber particle for (—) 5% (— —) 10%, (– – –) 15% rubber content.

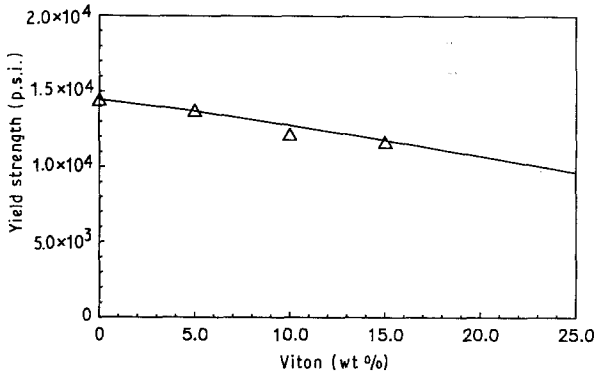

Figure 11 Composite yield strength as a function of rubber content for Ultem–Viton blends. (—) FEM, (△) experimental data.

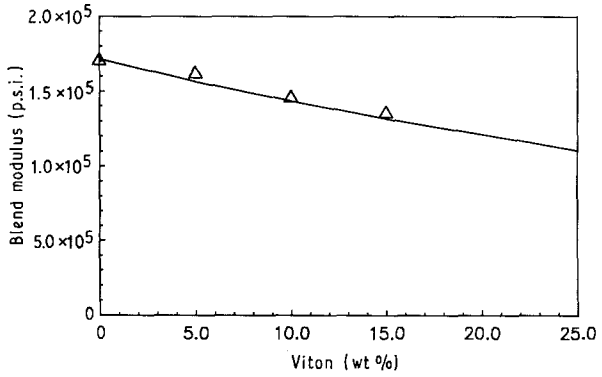

Figure 10 Composite modulus as a function of rubber content for Ultem–Viton blends. (—) FEM, (△) experimental data.

mer. These analyses will be compared with the experimental results of Furno and Nauman [15]. Blends of Ultem, a high-temperature thermoplastic (polyetherimide), with Viton, a heat-resistant fluoroelastomer, were produced by the process of compositional quenching. This process formed a dispersion of relatively uniform-sized spherical rubber particles of approximately 0.3 μm diameter. Blends containing 5, 10, and 15% by weight of Viton were produced. The elastic properties of Ultem and Viton are as follows

$$\text{Ultem:} \quad E = 1.716 \times 10^5 \text{ p.s.i.}$$
$$\nu = 0.35$$
$$\text{Viton:} \quad E = 1.0 \times 10^3 \text{ p.s.i.}$$
$$\nu = 0.48$$

Fig. 9 shows the interfacial stress intensity factor for the matrix as a function of position about the rubber particle for 5, 10, and 15% rubber volume fractions. An increase in rubber content causes an increase in stress magnification at the equator of the particle. Consequently, a lower applied stress is necessary to activate energy absorbing deformation processes in higher rubber content composites. This, in part, explains the increases in impact toughness found by Furno and Nauman [15] with increasing Viton content, because a larger volume of material would be experiencing a stress state sufficient to initiate a deformation process such as shear yielding. Fig. 10 compares the predicted blend modulus with the measured modulus of Ultem–Viton blends. The agreement between prediction and experiment is quite good. The predictive curves are based on the perfect adhesion assumption but are nearly identical to those found using the no adhesion assumption. Finally, Fig. 11 shows the predicted yield strength of Ultem–Viton blends as a function of rubber content. The results are compared with the experimental findings of Furno and Nauman [15]. The agreement is excellent. The matrix cross-section which first begins to yield is located approximately half the distance between the particle equator and the top of the particle. These results are consistent with experimental observation that shear bands originate at the particle surface approximately 45° from the particle equator [1].

4. Conclusions

A method for calculating the internal stresses in an elastic media that contains non-bonded spherical elastic inclusions is discussed. The numerical analysis used here accounts for interactions between particles unlike the pioneering work done by Goodier [2] but similar to the work done by Broutman and Panizza [3]. The use of a non-bonded inclusion in this model is in contrast to the work of many others [2–8] which assumed that perfect adhesion (continuity of displacement) exists between the particle and matrix. By considering both the no adhesion and perfect adhesion assumptions, we have established bounds on the real interfacial behaviour of the composite material.

For rubber-modified thermoplastics the stress state of the matrix when placed in tension is virtually independent of the adhesion between the matrix and inclusion. Thus, rubber inclusions are effective initiators of energy-absorbing deformation processes such as crazing and shear yielding, regardless of their degree of bonding to the matrix. These activated deformation processes are responsible for the enhancement in toughness observed under impact conditions. Whether the rubber particles increase the impact strength of a material due to initiating deformation processes depends on other factors related to the fracture mechanics of the composite. Specifically, the particles must not create a flaw of critical size such

that premature fracture instead of widespread deformation occurs. Flaws are present at the particle–matrix interface due to imperfect bonding. A completely non-bonded particle could result in a flaw of size equal to one-half the circumference of the particle. For polymers that deform primarily by shear yielding, such as nylon and Ultem, rubber particles below a certain size (for a given volume fraction of modifier) should be effective at increasing impact toughness since they would act as deformation initiators without providing critical flaws. This is consistent with Wu's [9] contention that shear yielding materials can be effectively impact-modified by rubber particles that are within some critical interparticle distance from one another. For materials that are impact-modified primarily through the action of crazing, the situation is more complicated. Although small non-bonded rubber particles may be effective initiators of crazes, they would be ineffective at terminating crazes as previously suggested by Bucknall [1] and thus cause critical flaws to be created as crazes propagate about particles. It would thus be expected that an optimum particle size range would exist for modifying crazing polymers which qualitatively would be particles large enough to terminate crazes and small enough so as to avoid providing critical flaws at the particle–matrix interface. In addition, the particles must be close enough so that the crazes formed between the particles are not larger than the critical flaw size. It would also be expected that interfacial adhesion plays a much larger role in composites that deform via crazing rather than shear yielding because a craze would propagate around the surfaces of poorly bonded particles.

The no adhesion assumption leads to some differences from the perfect adhesion assumption in predicted internal stresses. When the inclusion modulus exceeds the modulus of the matrix, the stress state of both the matrix and the inclusion are quite different depending on the interface assumption used. This leads to differences in calculated elastic properties such as the modulus and Poisson's ratio. These differences become significant when there is a large modulus mismatch between the two phases. Thus it is important to consider the interfacial condition of some modified materials such as filled ceramics or rubbers.

Although the two extremes in interfacial bonding have no impact on the calculated internal stresses of the matrix for rubber-modified polymers, the stresses within the rubber particle are quite different for the two situations. Because the elastic properties of the composite are primarily due to the behaviour of the matrix phase, the predicted elastic properties are essentially the same for the two interfacial conditions despite the differences in the particle stress state.

The finite element stress analysis provides an excellent means for predicting the elastic properties of a composite material. Only the volume fraction of modifier in the composite and not particle size is needed for the analysis. This is consistent with the observation that elastic properties, in contrast to impact properties, are relatively insensitive to differences in particle size [19]. Using the method described by Broutman and Panizza [3], the modulus calculated for Ultem–Viton blends containing various amounts of modifier is in excellent agreement with the experimental measurements of Furno and Nauman [15]. In addition, a method is proposed to calculate the yield strength of a rubber-modified polymer from the stress state of the composite. The agreement between prediction and experiment is again excellent.

References

1. C. B. BUCKNALL, "Toughened Plastics" (Applied Science, London, 1977).
2. J. N. GOODIER, *AMSE Trans.* **55** (1933) 39.
3. L. J. BROUTMAN and G. PANIZZA, *Int. J. Polym. Mater.* **1** (1977) 95.
4. S. H. LIU and E. B. NAUMAN, *J. Mater. Sci.*
5. M. E. J. DEKKERS and D. HEIKENS, *ibid.* **18** (1983) 3281.
6. V. A. MATONIS, *Polym. Engng Sci.* **9** (1969) 90.
7. *Idem, ibid.* **9** (1969) 100.
8. M. E. BOYCE, A. S. ARGON and D. M. PARKS, *Polymer* **28** (1987) 1680.
9. S. WU, *ibid.* **26** (1985) 1855.
10. D. R. PAUL and T. W. BARLOW, "Multiphase Polymers", ACS No. 176, Washington, DC (1976).
11. C. K. REIW, E. H. ROWE and A. R. SIEBERT, "Toughness and Brittleness of Plastics", ACS No. 154, Washington, DC (1976).
12. E. B. NAUMAN, M. ARIYAPADI, N. P. BALASARA, T. GROCELA, J. FURNO, S. LIU and R. MALLIKARJUN, *Chem. Engng Commun.* **56** (1988) 29.
13. S. NEWMAN, "Polymer Blends", Vol. 2 (Academic Press, New York, 1978) Ch. 13.
14. H. KESKKULO, in "Applied Polymer Symposium", No. 15 (New York, 1970), **15** (1970) 51.
15. J. S. FURNO and E. B. NAUMAN, *Polymer* **32** (1991) 88.
16. O. C. ZIENKIEWICZ, "The Finite Element Method" (McGraw-Hill, New York, 1967).
17. E. L. WILSON, *AIAA J.* **3** (1965) 2269.
18. B. D. AGARWAL and L. J. BROUTMAN, *Fibre Sci. Technol.* **7** (1974) 63.
19. J. S. FURNO and E. B. NAUMAN, *Proc. ACS Div. Polym. Mater. Sci. Engng* **61** (1989) 388.
20. T. T. WANG, M. MATSUO and T. K. KWEI, *J. Appl. Phys.* **42** (1971) 4188.
21. M. E. J. DEKKERS and D. HEIKENS, *J. Mater. Sci.* **19** (1984) 3271.

Received 26 September 1989
and accepted 9 April 1990